

Geometric Phase and Sidebands

Hualan Xu · Y.H. Ji · Z.S. Wang

Received: 31 August 2010 / Accepted: 26 October 2010 / Published online: 4 November 2010
© Springer Science+Business Media, LLC 2010

Abstract Geometric phase of mixed state is expanded for a two-level atom interacting with a quantized field mode, where master equation is a modified Bloch equation with constant terms that are used to explain emergence of sidebands in the spectrum of the fluorescent light. The results show that geometric phase transition is observed for medium initial angle when the Rabi frequency associated with the driving field becomes comparable to the spectral width of the atom. We find that the geometric phase transition depends on population inversion and Bloch radius, which is helpful to understand mechanism of sideband.

Keywords Geometric phase · Sideband · Modified Bloch equation

1 Introduction

The wave function of a quantum system retains a memory of its motion in terms of a geometric phase [1], which enable one to discern whether or not the system has undergone an evolution [2–4] by the geometric phase. This phase depends only on the area covered by the evolution of the system in parameter space and does not depend on how the motion is performed [5, 6]. The geometric phase factor can be measured in principle by interfering the wave function which has undergone the above evolution with another coherent wave function that did not evolve.

Application of geometric phases in quantum computation [7–11] has motivated people's studies to include decoherent effect [12–27]. In a real situation, The physical system is inevitably affected by uncontrollable degrees of freedom in the environment [28–30]. Differently from the pure state, the mixed state for the open system is always written in many different ways as a probabilistic mixture of distinct but not necessarily orthogonal pure states.

H. Xu · Y.H. Ji · Z.S. Wang (✉)

College of Physics and Communication Electronics, Jiangxi Normal University, Nanchang 330022,
People's Republic of China
e-mail: zishengwang@yahoo.com

Y.H. Ji · Z.S. Wang

Key Laboratory of Optoelectronic and Telecommunication of Jiangxi, Nanchang, Jiangxi 330022,
People's Republic of China

Thus, the density matrix was introduced as a way of describing the quantum open system and the state of the open system is not completely known. Up to now, therefore, the definition of the geometric phase for the open system is still a controversial issue. There have been many proposals tackling the problem from different generalizations of the parallel transport condition [12, 22]. However, a general belief is that the Berry phases are geometric in their nature, i.e., proportional to the area spanned in parameter space. Therefore, the geometric phase for the open system should be expressed here in terms of geometric structures on a complex projective Hilbert space [25–27]. Differently from the previous many works about the geometric phase within the conventional Bloch equation for the open system, especially, we consider here a modified Bloch equation that was used to explain sidebands in process of resonance fluorescence.

On the other hand, it is known that the current quantum computation presents a wide range of challenges to quantum information [31–33], particularly the search for devices of quantum memory that allow temporal storage of quantum information in a long distance quantum communication [34–36]. The sideband approach may be one of the available methods for quantum memory [37]. In addition to its fundamental importance for quantum processing and communications, the quantum memory promises a new tool for more precise experimental investigation of atom-photon interactions and the effective generation of new quantum states of light [38, 39]. Therefore, it is interesting to consider the geometric properties, which is a scheme intrinsically fault-tolerant and therefore resilient to certain types of computational errors.

2 Hamiltonian in Interacting Picture

The spectrum of resonance fluorescence provides an interesting manifestation of quantum theory of light, where a two-level atom is typically driven by a resonant continuous-wave laser field. When the Rabi frequency from the driving field becomes comparable to or larger than the spectral width of the atom, sidebands start emerging in the spectrum of the fluorescent light.

A physical understanding of this interesting phenomenon can be achieved by considering a dressed-atom picture of the atom-field interaction [40, 41]. The interaction Hamiltonian of a quantized field mode interacting with a two-level atom, in the rotating-wave approximation, is

$$\mathcal{H} = \mathcal{H}_0 + \mathcal{H}_1, \quad (1)$$

where $\mathcal{H}_0 = \frac{\hbar\omega}{2}\sigma_z + \hbar\nu a^\dagger a$ and $\mathcal{H}_1 = \hbar g(\sigma_+ a + a^\dagger \sigma_-)$. While a^\dagger and a denote the photon creation and annihilation operators satisfying the commutation relation $[a, a^\dagger] = 1$, σ_\pm are Pauli matrices and g is coupling constant between the two-level atom and driven field. It is convenient to work in the interaction picture. The Hamiltonian, in the interaction picture, is given by

$$\begin{aligned} \mathcal{H}_{int} &= \exp(i\mathcal{H}_0 t) \mathcal{H}_1 \exp(-i\mathcal{H}_0 t) \\ &= -\hbar g(\sigma_+ a e^{i(\omega-\nu)t} + \sigma_- a^\dagger e^{-i(\omega-\nu)t}). \end{aligned} \quad (2)$$

We will consider the case in which $\omega = \nu$ and therefore concerned only with Hamiltonian in the interacting picture, i.e.,

$$\mathcal{H}_{int} = \hbar g(\sigma_+ a + a^\dagger \sigma_-), \quad (3)$$

which has eigenstates,

$$|\pm, n\rangle = \frac{1}{\sqrt{2}}(|0, n\rangle \pm |1, n + 1\rangle), \tag{4}$$

with eigenvalues $\pm \frac{\hbar\Omega_R}{2}|\pm, n\rangle$ respectively. While $\Omega_R = 2\hbar g\sqrt{n + 1}$ is a Rabi frequency associated with the driving field. In order to simplify our calculations but without loss of generality, we assume that the field photon distribution has a sharp peak around the mean photon number so that the photon index n in the eigenstates is ignored. In the case, the basis may be rewritten as,

$$|0\rangle = \frac{1}{\sqrt{2}}(|+\rangle + |-\rangle), \quad |1\rangle = \frac{1}{\sqrt{2}}(|+\rangle - |-\rangle), \tag{5}$$

which is called as qubit. The Hamiltonian in the interacting picture and Pauli operators may be reexpressed by

$$\mathcal{H}_{int} = \frac{\hbar\Omega_R}{2}(|+\rangle\langle+| - |-\rangle\langle-|) \tag{6}$$

$$\sigma_- = |1\rangle\langle 0| = \frac{1}{2}(|+\rangle\langle+| + |+\rangle\langle-| - |-\rangle\langle+| - |-\rangle\langle-|), \tag{7}$$

$$\sigma_+ = |0\rangle\langle 1| = \frac{1}{2}(|+\rangle\langle+| - |+\rangle\langle-| + |-\rangle\langle+| - |-\rangle\langle-|). \tag{8}$$

3 Master Equation

The physical system is inevitably affected by uncontrollable degrees of freedom in the environment [28–30]. As a result of information about the dynamics of the system given by the time evolution of the density operator ρ , the dissipative dynamics of the qubits can be treated in the general framework of master equation. If each qubit interacts independently with its own environment, this leads to local decoherence and loss of correction between the qubits, i.e., Markovian approximation. The relevant physical condition for the Born-Markovian process is that the environment correlating time is small compared to the relaxation time of the system. Thus the master equation [42], in the Markovian process, can be expressed as

$$\dot{\rho} = -\frac{i}{\hbar}[\mathcal{H}_{int}, \rho] + \zeta\rho, \tag{9}$$

where

$$\zeta\rho = -\frac{\Gamma}{2}(\sigma_+\sigma_-\rho - 2\sigma_-\rho\sigma_+ + \rho\sigma_+\sigma_-), \tag{10}$$

is a superoperator, Γ is a decay rate. The first term of the master equation (9) is a unitary part of the systematic dynamics generated by the Hamiltonian \mathcal{H}_{int} in (3). The last term is a dissipative term of the systematic dynamics governed by the superoperator.

According to (6)–(10), Evolving equation of density may expressed as component forms, i.e.,

$$\dot{\rho}_{++} = \langle+|\dot{\rho}|+\rangle = -\frac{\Gamma}{2}\rho_{++} + \frac{\Gamma}{4}, \tag{11}$$

$$\dot{\rho}_{--} = \langle -|\dot{\rho}|- \rangle = -\frac{\Gamma}{2}\rho_{--} + \frac{\Gamma}{4}, \tag{12}$$

$$\dot{\rho}_{+-} = \langle +|\dot{\rho}|- \rangle = -\left(i\Omega_R + \frac{3\Gamma}{4}\right)\rho_{+-} - \frac{\Gamma}{4}\rho_{-+} - \frac{\Gamma}{2}, \tag{13}$$

$$\dot{\rho}_{-+} = \langle -|\dot{\rho}+ \rangle = -\left(-i\Omega_R + \frac{3\Gamma}{4}\right)\rho_{-+} - \frac{\Gamma}{4}\rho_{+-} - \frac{\Gamma}{2}, \tag{14}$$

which are a modified Bloch equation with constant terms if they are expressed by matrix form. Solution of (11)–(14) will be discussed at appendix. One finds

$$\rho_{--}(t) = \rho_{--}(0)e^{-\Gamma t/2} + \frac{1}{2}(1 - e^{-\Gamma t/2}), \tag{15}$$

$$\rho_{++}(t) = \rho_{++}(0)e^{-\Gamma t/2} + \frac{1}{2}(1 - e^{-\Gamma t/2}), \tag{16}$$

$$\begin{aligned} \rho_{+-}(t) = & \frac{1}{2\mu}(2\mu \cos \mu t - 2i\Omega_R \sin \mu t)e^{-3\Gamma t/4}\rho_{+-}(0) - \frac{\Gamma}{4\mu} \sin \mu t e^{-3\Gamma t/4}\rho_{-+}(0) \\ & + \frac{\Gamma}{2\mu} \left[\frac{2\mu(\Gamma/2 - i\Omega_R)}{\Gamma^2 + 2\Omega_R^2} \cos \mu t - \left(1 - \frac{(3\Gamma/2)(\Gamma/2 - i\Omega_R)}{\Gamma^2 + 2\Omega_R^2} \right) \sin \mu t \right] e^{-3\Gamma t/4} \\ & - \frac{\Gamma^2/2 - i\Gamma\Omega_R}{\Gamma^2 + 2\Omega_R^2}, \end{aligned} \tag{17}$$

$$\begin{aligned} \rho_{-+}(t) = & \frac{1}{2\mu}(2\mu \cos \mu t + 2i\Omega_R \sin \mu t)e^{-3\Gamma t/4}\rho_{-+}(0) - \frac{\Gamma}{4\mu} \sin \mu t e^{-3\Gamma t/4}\rho_{+-}(0) \\ & + \frac{\Gamma}{2\mu} \left[\frac{2\mu(\Gamma/2 + i\Omega_R)}{\Gamma^2 + 2\Omega_R^2} \cos \mu t - \left(1 - \frac{(3\Gamma/2)(\Gamma/2 + i\Omega_R)}{\Gamma^2 + 2\Omega_R^2} \right) \sin \mu t \right] e^{-3\Gamma t/4} \\ & - \frac{\Gamma^2/2 + i\Gamma\Omega_R}{\Gamma^2 + 2\Omega_R^2}, \end{aligned} \tag{18}$$

where $\mu = \sqrt{\Omega_R^2 - (\Gamma/4)^2}$ is relative to both the frequency from the driven field and the width of atom.

Using (15)–(18), it is easy to calculate the linewidths, where there is central component which goes as $\exp(-\Gamma t/2)$ and means a width $\Gamma/2$ of the central peak together with the two-frequency sidebands at $\pm\Omega_R$ having width $3\Gamma/4$.

4 Geometric Phase

It is known that quantum teleportation was successfully demonstrated by monitoring the squeezing with megahertz-order sidebands, which prevented signal from being polluted by low-frequency environmental noise. In particular, devices of quantum memory in current quantum information processing can be implemented by controlling two-frequency sidebands of a squeezed vacuum. Therefore, it is interesting to study geometric phase for process of two-frequency sidebands, where may have the built-in fault-tolerant advantage due to the fact that the geometric phases depend only some global geometric features.

At first, we expand the geometric phase from Refs. [25–27] to include the modified Bloch equation, which is embedded a geometric structure on a complex projective Hilbert space so

that the corresponding Berry phases for the mixed state are proportional to the area spanned in parameter space.

In order to obtain the geometric phase, firstly, three components of the Bloch vectors are defined as

$$u(t) = \rho_{+-}(t) + \rho_{-+}(t), \tag{19}$$

$$v(t) = i(\rho_{+-}(t) - \rho_{-+}(t)), \tag{20}$$

$$w(t) = \rho_{++}(t) - \rho_{--}(t), \tag{21}$$

which leads to a Bloch sphere structure and are parameterized by the radius $r(t)$ and two azimuthal angles $\alpha(t)$ and $\beta(t)$ of the Bloch sphere [25–27], i.e.,

$$r^2(t) = u^2(t) + v^2(t) + w^2(t), \tag{22}$$

which includes, differently from the usual open system within the Bloch equation, the contribution from the constant terms of the modified Bloch equation,

$$\alpha(t) = \cos^{-1} \frac{w(t)}{r(t)}, \tag{23}$$

and

$$\beta(t) = \tan^{-1} \frac{v(t)}{u(t)}. \tag{24}$$

It is noted that $w(t)$ is an important physical quantity to describe population inversion in process of physical evolution, while $r(t)$ quantify the mixed degree of physical state. when $r(t) = (u^2(t) + v^2(t) + w^2(t))^{1/2} = 1$, the Bloch vectors $(u(t), v(t), w(t))$ are points on this unit Poincaré sphere, which implies that the physical system is in a pure state at any evolving time.

For $r(t) = (u^2(t) + v^2(t) + w^2(t))^{1/2} < 1$, on the other hand, the Bloch vectors $(u(t), v(t), w(t))$ are interior points of this unit Poincaré sphere. It is known that the mixed states identify with the interior points of this sphere. From (20), it is proved that the Bloch radius is smaller than one in process of the dynamical evolution. Therefore, our physical system considered here is in the mixed state at all evolving time.

By renormalizing for the Bloch vectors, the interior points in the unit Poincaré sphere may be mapped onto field amplitudes as the mixed states $|\psi\rangle$ as pointed out by one of the authors [25], which may be expressed as

$$|\psi(t)\rangle = \left(\begin{array}{c} \sqrt{r} \cos \frac{\alpha(t)}{2} \\ \sqrt{r} \exp[i\beta(t)] \sin \frac{\alpha(t)}{2} \end{array} \right), \tag{25}$$

which includes the effect of atom interacting with its environment. Therefore, it is a dressed spin $-1/2$ state with nonunit vector in the complex projective Hilbert space.

It was known that the nonunit vector ray (25) in the projective Hilbert space is one-to-one correspondence with the Bloch vectors (19)–(21) [25]. Therefore, the approach from (25) to the geometric phase may be unique.

According to (25), the total phase of physical system is given by

$$\arg\langle\psi(t_0)|\psi(t)\rangle = \tan^{-1} \frac{\sin(\beta(t) - \beta(t_0)) \sin \frac{\alpha(t_0)}{2} \sin \frac{\alpha(t)}{2}}{\cos \frac{\alpha(t_0)}{2} \cos \frac{\alpha(t)}{2} + \cos(\beta(t) - \beta(t_0)) \sin \frac{\alpha(t_0)}{2} \sin \frac{\alpha(t)}{2}}, \tag{26}$$

and the geometric phase, expressed by the state vector in the complex projective Hilbert space, is obtained by [25–27],

$$\gamma_g = \arg\langle\psi(t_0)|\psi(t)\rangle - \Im \int_{t_0}^t \frac{\langle\psi(t)|d|\psi(t)\rangle}{\langle\psi(t)|\psi(t)\rangle}, \tag{27}$$

which is a gauge and reparameterized invariance [27, 43]. It is necessary to point out that (27) is a generalization for the Pantcharatnam formula in the pure state [44] and therefore is called as the Pantcharatnam phase of the mixed state [25]. It was proved that (27) was in agreement with the result directly from nonunitary evolution, where the geometric phase is expressed by the density matrix [25, 43]. It is interesting to note that, furthermore, under the transformation, $|\bar{\psi}(t)\rangle = \exp(-i \arg\langle\psi(t_0)|\psi(t)\rangle)|\psi(t)\rangle$, the geometric phase (27) may be rewritten as

$$\gamma_g^A = -\Im \int_{t_0}^t \frac{\langle\bar{\psi}(t)|d|\bar{\psi}(t)\rangle}{\langle\bar{\psi}(t)|\bar{\psi}(t)\rangle}, \tag{28}$$

which is a generalization of the Aharonov and Anandan phase of the pure state [45] with the condition of $\langle\bar{\psi}(t)|\bar{\psi}(t)\rangle = \langle\psi(t)|\psi(t)\rangle = 1$. Therefore, γ_g^A is called as the Aharonov and Anandan phase of mixed state.

Because of interacting with the environment, the system no longer undergoes a cyclic evolution, where the exponent decay factors are included in the density matrices, Bloch vectors and nonunit state vectors. When it is isolated from the environment, however, the evolving time $T = \frac{2\pi}{\Omega_R}$ in the quasicyclic process may be regarded as its cyclicity so that the total phase in (26) is equal to 2π , which is not important and may be dropped off in quantum computation. Thus, the geometric phase under the quasicyclic process may be expressed as

$$\begin{aligned} \gamma_g^B &= -\Im \int_0^T \frac{\langle\psi(t)|d|\psi(t)\rangle}{\langle\psi(t)|\psi(t)\rangle} \\ &= -\frac{1}{2} \int_0^T (1 - \cos \alpha(t)) d\beta(t), \end{aligned} \tag{29}$$

which is a generalized expression of the Berry phase of pure state and therefore is called the Berry phase of mixed state.

It is obvious that γ_g^B is an area in parameter space under the approximation of the quasicyclic evolution [27] and is accumulated at region of $t \in [0, T]$ in a quasicyclic evolution. While γ_g is a function of time associated with an evolution of a quantum open system [27, 45].

5 Discussions and Conclusions

In order to understand the physical processing of Berry phase, we suppose that the system evolves from a pure state at initial time to a mixed state at evolving time, i.e., $|\psi(t=0)\rangle = \cos\theta|+\rangle + \sin\theta|-\rangle$, where θ is an initial angle of the physical system.

The component w of Bloch vectors is shown at Fig. 1 as a function of decay rate for differently initial angles θ at point of quasicyclicity. We see that, for the smaller initial angles with $\theta = \pi/12, \pi/6$ and $\pi/5$, w decreases smoothly and varies from positive value $w > 0$ to $w = 0$. For the medium and larger initial angles with $\theta = \pi/3$ and $2\pi/3$, however,

Fig. 1 Population inversion w as a function of decay rate for differently initial angles θ at point of quasicyclicity

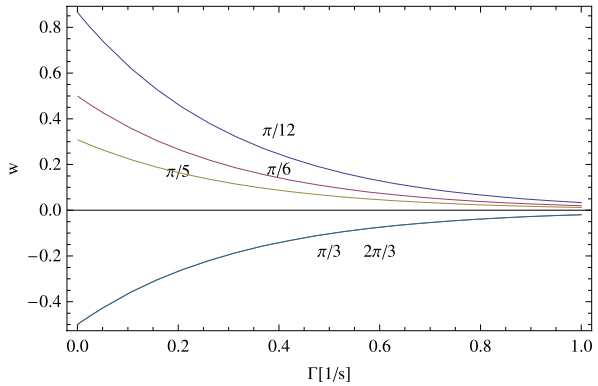
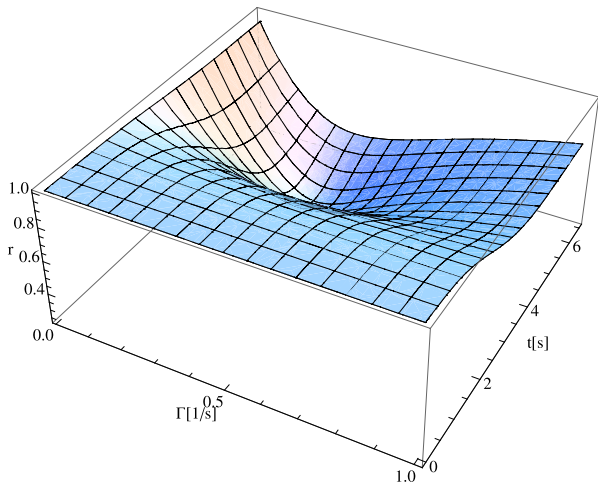


Fig. 2 Bloch radius $r(t)$ as functions of decay rate and evolving time with initial angle $\theta = \pi/3$



w increases smoothly and varies from negative value $w < 0$ to $w = 0$, where there are the same values for both $\theta = \pi/3$ and $\theta = 2\pi/3$. Therefore, w describes processing of population inversion in evolution of physical system.

From Figs. 2 and 3, we see that Bloch radius $r(t)$ describing the modified Bloch equation is different from that describing by the conventional Bloch equation without the constant terms, where the Bloch radius firstly decays and then increases with the evolving time because of the constant terms beyond the conventional Bloch equation.

It is noted that Bloch radiuses $r(t)$ with the initial angle $\theta = \pi/3$ and $\theta = 2\pi/3$ have the different ways of dynamical evolution with the evolving time and decay rate. We also find that the behaviors of dynamical evolution for small initial angles, i. e., $\theta = \pi/12, \pi/6$ and $\pi/5$, are similar to that of $\theta = \pi/3$.

Berry phase is shown at Fig. 4 as a function of decay rate for differently initial angles θ . We find that, for the smaller angles with $\theta = \pi/12, \pi/6$ and $\pi/5$ and the larger angle with $\theta = 2\pi/3$, Berry phases decrease smoothly at range of low decay rate and then trend constants because of constant terms of modified Bloch equation. However, it is interesting to note that the phase transition is taken place for the initial angle $\theta = \pi/3$ at the decay rate closed to $\Gamma = 0.3[1/s]$, where Berry phase is an increasing function of decay rate and a

Fig. 3 Same as Fig. 2 with initial angle $\theta = 2\pi/3$

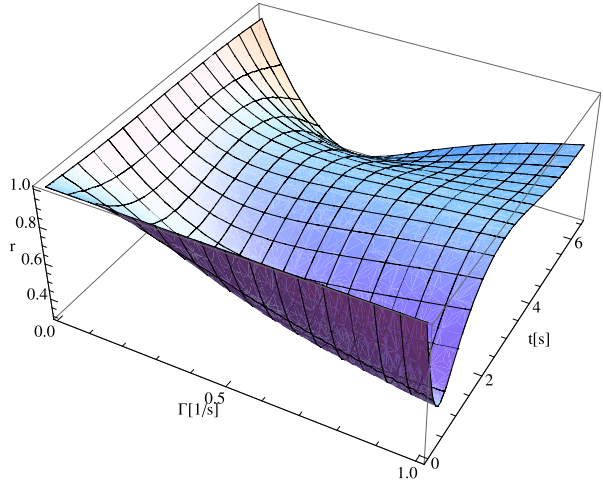
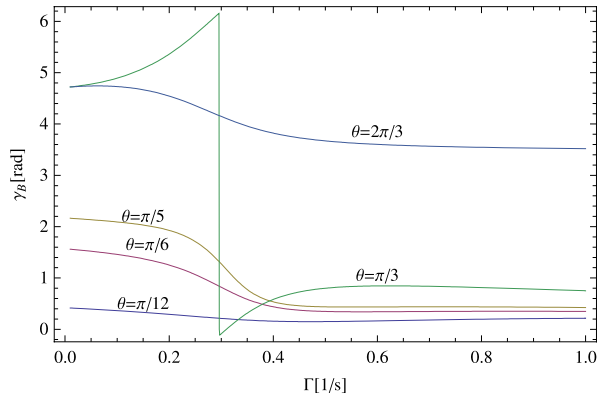


Fig. 4 Berry phase as a function of decay rate for differently initial angles θ



discontinuous point is emerged closed to $\Gamma = 0.3[1/s]$. Similar situations are found for the medium initial angles. In comparison with Figs. 1–3, it is obvious that the phase transition depends on both the population inversion and mixed degree.

The geometric phase transition may effectively explain sidebands in the spectrum of the fluorescent light, i.e., if the Rabi frequency associated with the driving field becomes comparable to the spectral width of the atom, sidebands will emerge. Since geometric phases are generally accompanied by dynamical ones which are not robust against local inaccuracies and fluctuations, it may be helpful for the sideband approach to quantum memory.

Acknowledgements This work is supported by the National Natural Science Foundation of China under Grant No. 10864002 and the Foundation of Science and Technology of Education Office of Jiangxi Province under Grant No. GJJ10404.

Appendix

Under the transformation,

$$\rho_{+-} = \tilde{\rho}_{+-} + c_{+-}, \tag{30}$$

$$\rho_{-+} = \tilde{\rho}_{-+} + c_{-+}, \tag{31}$$

$$\rho_{++} = \tilde{\rho}_{++} + c_{++}, \tag{32}$$

$$\rho_{--} = \tilde{\rho}_{--} + c_{--}, \tag{33}$$

where

$$c_{+-} = -\frac{\Gamma^2 - 2i\Gamma\Omega_R}{2(\Gamma^2 + 2\Omega_R^2)}, \quad c_{-+} = -\frac{\Gamma^2 + 2i\Gamma\Omega_R}{2(\Gamma^2 + 2\Omega_R^2)}, \tag{34}$$

(13) and (14) are rewritten by

$$\frac{d}{dt} \begin{pmatrix} \tilde{\rho}_{+-} \\ \tilde{\rho}_{-+} \end{pmatrix} = \begin{pmatrix} -i\Omega_R - \frac{3}{4}\Gamma & -\frac{\Gamma}{4} \\ -\frac{\Gamma}{4} & i\Omega_R - \frac{3}{4}\Gamma \end{pmatrix} \begin{pmatrix} \tilde{\rho}_{+-} \\ \tilde{\rho}_{-+} \end{pmatrix}, \tag{35}$$

which has eigenvalues,

$$\lambda_1 = \frac{1}{4}(-3\Gamma + \sqrt{\Gamma^2 - 16\Omega_R^2}) = -\frac{3\Gamma}{4} + i\mu, \tag{36}$$

$$\lambda_2 = \frac{1}{4}(-3\Gamma - \sqrt{\Gamma^2 - 16\Omega_R^2}) = -\frac{3\Gamma}{4} - i\mu, \tag{37}$$

and corresponding Eigenvectors,

$$\begin{pmatrix} i \sin \chi \\ \cos \chi \end{pmatrix}, \quad \begin{pmatrix} i \cos \chi \\ \sin \chi \end{pmatrix}, \tag{38}$$

where $\tan \chi = \frac{\Omega_R - i\mu}{\Gamma/4}$. Thus the solution to (35) may be constructed by

$$\begin{pmatrix} \tilde{\rho}_{+-} \\ \tilde{\rho}_{-+} \end{pmatrix} = c_1 e^{\lambda_1 t} \begin{pmatrix} i \sin \chi \\ \cos \chi \end{pmatrix} + c_2 e^{\lambda_2 t} \begin{pmatrix} i \cos \chi \\ \sin \chi \end{pmatrix}, \tag{39}$$

where c_1 and c_2 is determined by initial condition. We find

$$c_1 = \frac{\cos \chi \rho_{-+}(0) + i \sin \chi \rho_{+-}(0)}{\cos 2\chi} - \frac{c_{-+} \cos \chi + i c_{+-} \sin \chi}{\cos 2\chi}, \tag{40}$$

$$c_2 = -i \frac{\cos \chi \rho_{+-}(0) - i \sin \chi \rho_{-+}(0)}{\cos 2\chi} + i \frac{c_{+-} \cos \chi - i c_{-+} \sin \chi}{\cos 2\chi}. \tag{41}$$

Inserting (40) and (41) into (39), then using (30)–(31) and (34), we find that the solutions of (13) and (14) may be expressed as (17) and (18). A similar situation is for the solutions of (11) and (12), which are given by (15) and (16).

References

1. Berry, M.V.: Proc. R. Soc. A **392**, 45 (1984)
2. Suter, D., Mueller, K.T., Pine, A.: Phys. Rev. Lett. **60**, 1218 (1988)
3. Bhandari, R., Samuel, J.: Phys. Rev. Lett. **60**, 1211 (1988)
4. Chiao, R.L., et al.: Phys. Rev. Lett. **60**, 1214 (1988)
5. Simon, B.: Phys. Rev. Lett. **51**, 2167 (1983)
6. Wang, Z.S., et al.: Phys. Scr. **75**, 494 (2007)
7. Wang, Z.S., Kwek, L.C., Lai, C.H., Oh, C.H.: Phys. Lett. A **359**, 608 (2006)
8. Wang, Z.S., Wu, C., Feng, X.-L., Kwek, L.C., Lai, C.H., Oh, C.H., Vedral, V.: Phys. Lett. A **372**, 775 (2008)
9. Wang, Z.S., Wu, C., Feng, X.-L., Kwek, L.C., Lai, C.H., Oh, C.H., Vedral, V.: Phys. Rev. A **76**, 044303 (2007)
10. Wang, Z.S.: Phys. Rev. A **79**, 024304 (2009)
11. Wang, Z.S., Liu, G.Q., Ji, Y.H.: Phys. Rev. A **79**, 054301 (2009)
12. Uhlmann, A.: Rep. Math. Phys. **24**, 229 (1986)
13. Samuel, J., Bhandari, R.: Phys. Rev. Lett. **60**, 2339 (1988)
14. Ellinas, D., Dupertuis, S.M., Dupertuis, M.A.: Phys. Rev. A **39**, 3228 (1989)
15. Dattoli, G., Mignani, R., Torre, A.: J. Phys. A **23**, 5795 (1990)
16. Sjöqvist, E., Pati, A.K., Ekert, A., Anandan, J.S., Ericsson, M., Oi, O.K.L., Vedral, V.: Phys. Rev. Lett. **85**, 2845 (2000)
17. Carollo, A., Fuentes-Guridi, I., Franca Santos, M., Vedral, V.: Phys. Rev. Lett. **90**, 160402 (2003)
18. Fonseca Romero, K.M., Aguiar, A.C., Thomaz, M.T.: Physica A **307**, 142 (2002)
19. Nazir, A., Spiller, T.P., Munro, W.J.: Phys. Rev. A **65**, 042303 (2003)
20. Whitney, R.S., Gefen, Y.: Phys. Rev. Lett. **90**, 190402 (2003)
21. De Chiara, G., Palma, M.: Phys. Rev. Lett. **91**, 090404 (2003)
22. Tong, D.M., Sjöqvist, E., Kwek, L.C., Oh, C.H.: Phys. Rev. Lett. **93**, 080405 (2004)
23. Whitney, R.S., et al.: Phys. Rev. Lett. **94**, 070407 (2005)
24. Carollo, A., et al.: Phys. Rev. Lett. **96**, 150403 (2006)
25. Wang, Z.S., et al.: Europhys. Lett. **74**, 958 (2006)
26. Wang, Z.S., et al.: Phys. Rev. A **75**, 024102 (2006)
27. Wang, Z.S.: Int. J. Theor. Phys. **48**, 2353 (2009)
28. Chen, Z.Q., Guo, L.P., Chen, Y., Li, X.L., Liu, G.Q., Ji, Y.H., Wang, Z.S.: Int. J. Theor. Phys. **49**, 18 (2010)
29. Wang, Z.S., Wang, J., Jiang, Y., Chen, Z.Q., Ji, Y.H.: Adv. Stud. Theor. Phys. **4**, 241 (2010)
30. Rao, H.-Y., Hu, L.-Y., Liu, G.Q., Wang, Z.S.: Int. J. Theor. Phys. **49**, 1396 (2010)
31. Barenco, A., Deutsch, D., Ekert, A., Jozsa, R.: Phys. Rev. Lett. **74**, 4083 (1995)
32. Bennett, C.H., DiVincenzo, D.P.: Nature (London) **404**, 247 (2000)
33. Biolatti, E., Iotti, R.C., Zanardi, P., Rossi, F.: Phys. Rev. Lett. **85**, 5647 (2000)
34. Moiseev, S.A., Arslanov, N.M.: Phys. Rev. A **78**, 023803 (2008)
35. Gisin, N., Moiseev, S.A., Simon, C.: Phys. Rev. A **76**, 014302 (2007)
36. Staudt, M.U., et al.: Phys. Rev. Lett. **98**, 113601 (2007)
37. Furusawa, A., Kozuma, M.: Phys. Rev. A **81**, 021605 (2010)
38. Moiseev, S.A., Tittel, W.: In: Workshop on the Storage and Manipulation of Quantum Information in Optically-Addressed Solids, Bozeman, Montana, January 25–27, 2008
39. Underwood, M.S., Marzlin, K.-P., Tittel, W.: In: Workshop on the Storage and Manipulation of Quantum Information in Optically-Addressed Solids, Bozeman, Montana, January 25–27, 2008
40. Scully, M.O., Zubairy, M.S.: Quantum Optics. Cambridge University Press, Cambridge (1997)
41. Mollow, B.R.: Phys. Rev. **188**, 1969 (1969)
42. Lindblad, G.: Commun. Math. Phys. **48**, 119 (1976)
43. Mukunda, N., Simon, R.: Ann. Phys. (N.Y.) **228**, 205 (1993); 269 (1993)
44. Pancharatnam, S.: Proc. Indian Acad. Sci. A **44**, 1225 (1956)
45. Aharonov, Y., Anandan, J.: Phys. Rev. Lett. **58**, 1593 (1987)